A framework for the probabilistic analysis of PEMFC performance based on multi-physical modelling, stochastic method, and design of numerical experiments

Nicolas Noguer, Denis Candusso, Raed Kouta, Fabien Harel, Willy Charon, Gerard Coquery

A framework for the probabilistic analysis of PEMFC performance based on multi-physical modelling, stochastic method, and design of numerical experiments

N. Noguer [1, 2, 3], D. Candusso [3, 4*], R. Kouta[1, 2], F. Harel [4, 5], W. Charon [1], G. Coquery [3]

[1] UTBM / IRTES / M3M, Rue de Leupe, F 90400 Sévenans, France
[2] FCellSYS, UTBM bâtiment F, Rue Thierry Mieg, F 90010 Belfort Cedex, France
[3] IFSTTAR / COSYS / SATIE (UMR CNRS 8029), 25 Allée des marronniers, F 78000 Versailles Satory, France
[4] FCLAB (FR CNRS 3539), UTBM bâtiment F, Rue Thierry Mieg, F 90010 Belfort Cedex, France
[5] Université de Lyon, IFSTTAR / AME / LTE, 25 Avenue François Mitterrand, Case24, Cité des mobilités, F-69675 Bron Cedex, France

* Corresponding author:
denis.candusso@ifsttar.fr

Tel: 0033 3 84 58 36 33
Fax: 0033 3 84 58 36 36

Other email addresses:
nicolas.noguer@utbm.fr
raed.kouta@utbm.fr
fabien.harel@ifsttar.fr
willy.charon@utbm.fr
gerard.coquery@ifsttar.fr

Abstract
In this article, a probabilistic approach is applied to evaluate the impact of the GDL porosity uncertainty on the electrical performances of a PEMFC. The study is based on the use of a dynamical, symbolic, and acausal knowledge model. Some statistical distributions are introduced on the input model parameter (porosity) and the statistical distributions induced on the output parameters (cell voltage, resistance) are analyzed. The difference observed between the shapes of the input and output distributions (respectively some Gaussian and inverse Gamma distributions with a threshold phenomenon) is the result of strong nonlinearities linked with the integration of multiphase flow phenomena in the modelling (e.g. diffusion limit of the humidified air in the GDL). The study is also conducted for different conditions of temperature and pressure through a design of numerical experiments. One of the results obtained is that the variation coefficient related to the GDL porosity has, compared to the other parameters with their intervals of variation considered, little effect on the average output distributions. However, the dispersion introduced on the porosity impacts their shapes (e.g. significant effect on the standard deviation).

Keywords:
PEM fuel cell; reliability; statistical analysis; design of experiments

Highlights:
• Probabilistic approach for the analysis of fuel cell performance and reliability.
• Integration of uncertainty on GDL porosity into a knowledge PEMFC model.
• Uncertainty on porosity represented by Gaussian probability distributions.
• Inverse Gamma distributions with threshold phenomenon observed for voltage outputs.
• Significant impact of GDL porosity dispersion on shapes of voltage distributions.

1. Introduction

Proton exchange membrane fuel cell (PEMFC) systems receive much attention as potential alternative sources of power generation for transport [1], stationary and portable applications [2]. Nevertheless, lower costs and higher durability are still needed for the deployment of the technology on a larger commercial scale. Numerous research activities are currently devoted to Fuel Cell (FC) ageing and degradation issues with the aim to enhance the system lifetime. Different cell ageing causes and mechanisms are discussed in the review articles dealing with MEA (Membrane Electrode Assembly) degradation: for instance, degradation of catalyst metal and carbon-support- corrosion inducing a reduction of electrode active surface area [3], membrane failures with increased crossover of the reactant gases from through-thickness cracks or pinholes which are formed by a combination of chemical and mechanical degradation during FC operation [4], contamination and poisoning mechanisms [5].
Reliability is another key-point that needs to be considered for a widespread marketing of FC stacks. The FC reliability is usually considered as the likelihood that the FC will not fail without maintenance, repair and overhaul within a specific time period [6].
For a given application, the selections of the different materials used in the various components of the FC, the choices in the FC design (geometrical characteristics / sizes of the cell components) correspond to tradeoffs between maximal electrical performances, minimal fuel consumption, high lifespan and reliability targets, and minimal costs. In any case, it is necessary to identify the FC design parameters and the operating conditions that maximize the cell performance with minimum variability. It is important to ensure at least a minimal cell performance level (e. g. a minimal cell voltage threshold) that can be considered as sufficient to meet the application requirements.

To assess the reliability of a FC (single cell, complete stack or stack segment), some specific analysis approaches combined with adapted modeling and simulations tools can be developed successfully. Mawardi et al. [7] proposed a methodology based on a one-dimensional non isothermal description of the governing physical phenomena and sampling-based stochastic model in order to analyze the interactive effects of parameter uncertainty on the performance of a PEMFC. In their work, Mawardi et al. proposed a remarkable mathematical framework incorporating the interactive effects of parameter uncertainty on the performance of the FC, which is necessary for a realistic, physics-based simulation and robust design. However, the model of the PEMFC used in this work was mainly based on single-phase flow descriptions and thus, it did not take into account the strong linearity induced by multi-phase flow descriptions. A multi-phase flow description (where each reactant is considered as a mix of gases interacting with liquid water) would increase the interest of developing a stochastic approach.
Naga Srinivasulu et al. [8] used a multi-parametric sensitivity analysis to investigate PEMFC electrochemical models with the aim to determine the relative importance of each model parameter on the simulation results. Although the analysis of Naga Srinivasulu et al. was not done in the framework of a stochastic approach, as it was proposed by Mawardi et al., the results allow evaluating the importance of each model parameter with respect to the simulation accuracy and thus, they can be helpful to FC designers and manufacturers.
In [9, 10], Placca et al. used a full factorial design and a statistical sensitivity analysis (Analysis of variance - ANOVA) to estimate the effects and contributions of model parameters subject to uncertainty on the computed output voltage. The model used for this study was a semi-empirical FC model giving a unique equation that links the voltage delivered by a cell to the input parameters. So, the model adopted in this work was rather simple but the uncertainty was integrated on model parameters through probability distributions, in a similar way to [7].

In [11], Wei Yuan et al. studied the effects of operating parameters (e.g. operating pressure, FC temperature, relative humidity of reactant gases, and air stoichiometric ratio) on the performance of the FC by using a three-dimensional, multi-phase, typical nine-layer model. A commercial Computational Fluid Dynamics (CFD) software package was used to solve this predictive model. The modeling results obtained for various operating conditions were illustrated and compared through polarization curves. No stochastic framework (i.e. no variation of parameters through probability distributions) was proposed in this work.
M. Noorkami et al. [12] used Monte-Carlo stochastic samples on a simple lumped mathematical model to focus on the effect of temperature incertitude, under different operational conditions, on FC performance. Some of the assumptions applied for the modelling were: steady state system, single phase vapor water; no pressure drop. A statistical approach, using Monte Carlo stochastic sampling, was developed. A "probability map" of PEMFC polarization behavior was provided through the definition of a polarization "area" or "band" as opposed to a simple polarization "curve".
In [13], M. Kerdi et al. proposed to use a generalized steady-state electrochemical FC model (based on the works of Fowler et al. [14]) and to integrate some degradation mechanisms from the literature. In their paper, M. Kerdi et al considered a random temperature following a normal distribution and analyzed its effect on the MEA behavior. Then, a probabilistic analysis was conducted, based on a Monte Carlo simulation of the FC behavior, and using the FC voltage and lifespan parameters. The probability distributions of these parameters were deduced. The work of Kerdi et al. was intended to help identifying some components likely to break down and proposing some well-suited maintenance policy.
More recently, M. Whiteley et al. [15] have adopted Petri-Net simulation and FC modelling techniques to develop an accurate degradation model. Operational parameters and their effects on the occurrence of failure modes could be modelled through this technique. The work is intended to improve previous FC reliability studies by taking into consideration operating parameters (water content, temperature, load current), FC voltage based on user demand (drive cycles), and dependencies between failure modes.
As stated by Weber et al. in their review article [16] in the Section entitled "Modeling Stochastic and Statistical Performance", there is a variability to experiments that should be represented in modeling. For example, the experiments show a natural variability due not only to the component variability but also to the fluctuations in operating conditions. The models should account for these variations in terms of detailed sensitivity studies and it becomes of interest to study the numerical prediction of the cell performance from a similar statistical basis. In [16], Weber et al. shows, as an example of study, a typical variation of Gas Diffusion Layer (GDL) thickness, determined by statistical parameters, and its effects on the cell polarization curve shape.

In [17, 18], we propose the baselines of a novel method to help evaluating the reliability of a PEMFC stack. The aim is to guarantee a target level of electrical performance. The approach is based on the close coupling between physical modeling and statistical analysis of reliability. The complexity of the physical phenomena involved in the FC is taken into account through the development of a dynamical, symbolic, acausal modeling tool including physical and semi-empirical parameters as well.
A detailed description of our new PEMFC multi-physical model is available in [17, 18]. Some temporal simulation results were also presented with two aims:

- to compare the simulation results obtained with some experimental data acquired on a FC test bench,
- to highlight some of the possibilities offered by our dynamical model that intends to take into account the complexity of the water management inside the different cell parts.

The proposed knowledge PEMFC model is one-dimensional, non-isothermal, but it includes a two-phase fluidic flow representation (each reactant is considered as a mix of gases and liquid water). The modeling is implemented using the MODELICA – DYMOLA environment; one of the advantages of this simulation tool is that it allows an effective connection between multi-physical modeling and statistical treatments.

In this article, we will first propose a synthetic overview of our new PEMFC multi-physical and dynamical model (Section 2). Then, we will give a concise overview of the proposed probabilistic approach in which our knowledge model is used to model the consequences of the parameter uncertainty on the FC performances (Section 3). In this paper, we will study, as an example of statistical and reliability engineer analysis, the effect of the GDL porosity uncertainty on the electrical performances of a single cell PEMFC (Section 4). The variation of the GDL porosity parameter is an interesting example: the variations introduced on its value are likely to be caused by mechanical stress that can be included in further modeling developments based on the works of [19-21]. In this paper, we will show how some statistical distributions can be introduced on the input model parameter and how the statistical distributions induced on the output parameters quantifying the FC performance (cell voltage or FC resistance) can be analyzed. Some physical interpretations will be given for the shapes of the statistical distributions observed on the model output (i.e. cell voltage) and intermediate computing results (e.g. partial pressures in the FC model layers). In Section 5, we will study the impact of uncertainty (still linked with the cathode porosity) on the FC performance (FC voltage and resistance) in different operating conditions (for various cell temperature and pressure levels). The analyses will be conducted through a design of numerical experiments, and with the use of various tools (graphs of the effects, graphs of the coefficients of variation). The aim is to highlight the effect of the input parameter (GDL porosity) variation on the shapes of the output (voltage) distributions. Finally, the article will be completed by major conclusions and outlooks (Section 6).

2. Multi-physical modelling

In this section, we propose a global description of our new PEMFC multi-physical model. The simulation tool has been developed in the MODELICA – DYMOLA environment and the computing results have been confronted to experimental tests. A detailed description of the modeling developed to describe the different physical phenomena (notably related with diffusion and mass transport processes) can be found in [17]. In this previous article, some temporal simulation results were also presented with the aim to highlight some of the possibilities offered by the dynamical model that intends to take into account the complexity of the water management inside the different cell parts.
In our work [18], the modeling concerns a whole individual cell of a FC stack. The cell is divided into nine parts: two active layers (catalyst layers), two diffusion layers, two bipolar (or monopolar) plates, two current collector plates and one membrane. Figure 1 shows the graphical multi-layer representation of a single PEMFC using the DYMOLA software developed by Dassault Systèmes [22] that brings a graphical interface to the MODELICA language [23]. This modeling environment has been selected to conduct our work for two main reasons. First, it offers the possibility to create some libraries of component models that can be used in a modular way to generate some multi-physical models. Second, it integrates a specific module that facilitates the creation of variations on one or several input parameters in the model according to statistical distributions which traduce different types of uncertainty to be taken into account (Section 4).

Gas feeding section

Multi-species

Cathode: O_2+N_2 + Water vapor

Anode: H_2 + Water vapor

⇨ With ≠ T, P, %RH, stoichiometry rates at anode and cathode

Electrodes

Chemical reactions

H_2O production (vapor)

Heat exhaust / absorption

Electrical potential computing

Gas diffusion

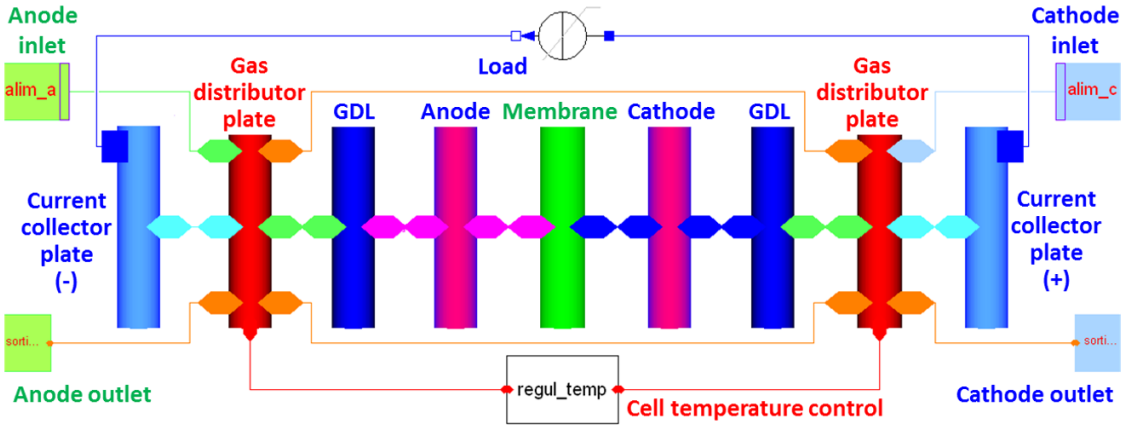

Gas Diffusion Layers (GDL)

Knudsen diffusion

Stephan-Maxwell equations

(diphasic gas mix: liquid + vapor water)

Membrane

Electro-osmose

Absorption

Back-diffusion

Fig. 1. First model layer of the PEMFC simulated in the DYMOLA environment. Examples of key physical phenomena considered in different model sub-layers.

Such a single cell model can be assembled with other cell models to obtain a complete stack representation. In our work, a global approach has been considered to develop the model that allows knowing the temporal evolution of the variables related with each cell element. The local conditions in the cell model sections are dynamically computed using classical mass balance and transport laws, energy conservation relations that can be found for instance in [24, 25].
In a first step, the principle of our modeling approach is to create a model containing as much physical parameters as possible, such as the porosities of diffusion layers or active surfaces, in order to be able to observe the effects of these parameter values on the electrical responses of the cell, and more globally on the physical behaviors of the FC. In its current stage of development, the FC model includes more than 500 variables and equations [17].

The cell modeled is fed by humidified air and hydrogen flowing through the channels of the gas distribution plates at cathode and anode sides respectively. The reactants cross the GDLs and reach the electrode active zones. The load current is imposed to the cell and the electrical potentials at the electrodes are computed as a function of the concentrations of reactants; they are also dependent on the temperatures in the catalyst layers. The model calculates the electrical voltage between the cell terminals by taking into account the voltage drops linked with the different zones / layers of the cell. Each cell layer is governed by its own physical phenomena

resulting in possible electrical losses. For example, in the GDLs, diffusions of multi-specie and multi-phase gases are considered with diffusion overvoltages as a consequence (the diffusion is represented according to [26] through well-suited modelling analogies between electrical and fluidic behaviors, between electronic and thermal conductions). The cell voltage can be computed for various operating conditions linked with the different types of parameters to be studied:

- FC operating parameters (cell temperature, stoichiometric coefficients and pressures of the reactants, humidity rates of the gases at cell inlets). It will be possible to evaluate the effects of these parameters on the cell electrical response by analyzing temporal and/or statistical responses (see [17] and Sections 4 - 5).
- Intrinsic parameters (such as the thicknesses of the assembly layers or the GDL material porosity). As for FC operating parameters, it will be possible to evaluate the impacts of the intrinsic parameters on the cell response through temporal and/or statistical analyses.
- The model will also allow identifying the impacts of semi-empirical parameter values which are possibly used in semi-physical relations linked with particular zones of the model (e.g. activation coefficients of the FC current - voltage law, which are usually represented through α or β coefficients [17]). Comparisons with experimental data and sensitivity analyses will allow finding adapted values for these parameters or neglecting some of them.

Note that, in the different possible parameter studies, some transient states can be observed using the model; the influence of phenomena with constant times higher than 0.1 s about can be considered.

The main simplifications and hypotheses considered in the current development state of the model are the following ones:

- usual ranges of operating conditions are considered (e.g. FC temperature varies between 20 and 85°C).
- gases are ideal mixtures and fluidic flows are considered laminar,
- mass and charge transports are one-dimensional,
- temperature is uniform in a layer of the cell assembly,
- catalytic layers include both carbon and platinum layers,
- mechanical behaviors [27] and electrical contacts [28] are not yet taken into consideration but the model structure should allow their future implementations. We notably intend to integrate some mechanical behaviors in further developments and some of the results obtained by our lab in this field (in particular recent results obtained from the ex-situ GDL characterizations [27] [28]).

As mentioned before, the mixture gas is in a multi-phase state. In each layer, the water is present under gas or liquid form, and the equilibrium between the two phases depends mainly on the water saturation pressure and water gas pressure. The vapor water produced in the catalyst area at cathode condenses into liquid water or diffuses through the GDL, and evacuates. Vapor water, electrons, protons and heat result from the chemical reactions. As already stated, through the global cell model, the temperature is neither constant nor homogenous; however, it is uniform in each layer of the cell assembly. In the cathode layer, the heat produced propagates into the complete cell. The anodic side consumes a part of the thermal energy produced to dissolute hydrogen. A basic cooling system is modeled to regulate the temperature on the outlet of the FC cooling circuit.

As already mentioned, a more detailed description of the model developed can be found in [11]. Below, we only recall the equations of the sub-model used for the computing of the steady-state electrical law: FC voltage (U) vs. FC load current characteristics indexed on the oxygen and

hydrogen pressures at the electrode interfaces (p_{O_2} and p_{H_2}), and on the electrode temperatures (T). Many works use such an electrical sub-model alone, i.e. without any additional integration into a more complex fluidic and thermal model. In the next sections of the paper, this semi-empirical sub-model will be qualified as "simple" model.

$$U(I) = E_{rev} - I \cdot R_m + \beta_1 + \beta_2 \cdot T + \beta_3 \cdot T \cdot \ln(I/A_{cell}) + \beta_4 \cdot T \cdot \ln([O_2]) + \beta_5 \cdot T \cdot \ln([H_2]) \quad (1)$$

With:

$$E_{rev} = E_{max} + 4.3085 \cdot 10^{-5} \cdot T \cdot [\ln(p_{H_2}/p_{H_2O}) + 0.5 \ln(p_{O_2}/P_0)] \quad (2)$$

$$E_{max} = 1.229 - 0.85 \cdot 10^{-3}(T - 298.15) \quad (3)$$

$$[O_2] = \frac{p_{O_2}}{5.08 \times 10^5 \times e^{\frac{-498}{T}}} \quad (4)$$

$$[H_2] = \frac{p_{H_2}}{1.09 \times 10^5 \times e^{\frac{77}{T}}} \quad (5)$$

The membrane proton conductivity can be calculated according to a semi-empirical relation. The resistance of the membrane is computed from its proton conductivity (σ_m) and surface (A_{cell}).

$$\sigma_m = (a\lambda - b) \cdot exp\left[c\left(\frac{1}{303} - \frac{1}{T}\right)\right] / Cadj \quad (6)$$

$$R_m = e_m/(A_{cell} \cdot \sigma_m) \quad (7)$$

The values of the parameters and semi-empirical coefficients (β, a, b, c, and Cadj) used in the equations (1) to (7) can be found below.

$$\beta_1 = -0.966$$
$$\beta_2 = 0.003307$$
$$\beta_3 = -0.000135$$
$$\beta_4 = 0.0001342$$
$$\beta_5 = 0.0000677$$
$$A_{cell} = 0.022\ m^2$$
$$P_0 = 100000\ Pa$$
$$a = 0.5139$$
$$b = 0.326$$
$$c = 1268$$
$$Cadj = 7.5$$
$$e_m = 30 \cdot 10^{-6}\ m$$

The values of these coefficients have been found in the literature [14] and adjusted so that the simulated FC current-voltage curves can match with different experimental tests performed in the laboratory on a PEMFC stack manufactured by the CEA LITEN in Grenoble (France) and dedicated to automotive applications [17].

The cell is modeled with the physical parameters given in Table 1 (which are actually the main cell dimension parameters) while the nominal operating conditions of the FC are reported in Table 2. The modeled FC has some characteristics which are close to those of the experimented PEMFC stack.

Table 1. Cell characteristics.

Parameter	**Value**	**Units**
Active area	0.022	m^2
Membrane thickness	30.10^{-6}	m
Active layer thickness	50.10^{-6}	m
GDL thickness	180.10^{-6}	m
Stainless steel plate thickness	1.10^{-3}	m

Table 2. Cell nominal operating conditions.

Parameter	**Value**	**Units**
Load current	110	A
Cell temperature	80	°C
Inlet gas temperature	80	°C
FC inlet pressure	1.5	MPa
Stoichiometric coefficient at cathode	2	[-]
Stoichiometric coefficient at anode	1.5	[-]
Relative humidity at anode and cathode (for a temperature of 80°C)	50	%

Some examples of comparisons between experimental records and temporal simulations are available in [17, 18]. A good correlation between the model outputs and the stack output performances (voltages, membrane resistances) was noticed both in steady-state operations and with a load current profile described in [17, 18].
At this stage of the FC model development, the primary objective was: - first to obtain some qualitative simulation results that could represent some typical behaviors of PEMFC operated in various conditions (deviations of cell temperature; gas pressures, flows, and relative hygrometry rates from the nominal conditions), - second, to have a model that can be used as a basis to develop a framework for the probabilistic analysis of PEMFC performance based on multi-physical modelling, stochastic method, and design of numerical experiments.

3. Guidelines for the integration and analysis of parameter uncertainties into the deterministic model.

In this section, we provide some essential information about the method used to integrate and analyze some parameter uncertainties into our FC knowledge model. Figure 2 provides a synopsis of the adopted method with its different steps: from the model development phase (including the confrontation with some test results) to the reliability analysis sequence (using designs of numerical experiments).

As already mentioned in [17], the DYMOLA software includes a specific module that facilitates the creation of variations on one or several parameters in the model according to different statistical laws. The statistical analyses can be of two types:

- Simulation of a statistical sample according to a theoretical distribution generated by the Monte-Carlo method,
- Probabilistic modeling of a statistical sample that aims to represent the consequences of the uncertainty injected into the FC physical model.

The statistical analysis is based on numerical simulations obtained through the physical model that includes uncertain parameters. The method allows quantifying the uncertainty levels of the parameters, observing the propagation of the uncertainties through a determinist model, and analyzing the output parameters in order to determine the robustness and reliability of the FC. The uncertainties can be described by different probability laws which have to be selected according to the nature considered for the uncertainty. Three scenarios are possible:

- A Gauss Law (or Normal Law) for an optimistic or optimal uncertainty,
- A Uniform Law for a non-controlled uncertainty, or for a pessimistic uncertainty,
- A Gamma Law (or Weibull Law) for an uncertainty that can be considered as a "realistic" one.

The Monte-Carlo method is used for the simulation of the statistical sample that aims to represent the parameter considered as uncertain. For each simulation, the multi-physical FC model computes a response and, after a given number of simulations, a distribution can be generated as an output [7]. The number of simulations used to produce the distributions allows avoiding any bias (due to numerical noise) in the obtained results. The last step consists in analyzing the output distribution using suitable tools (e.g. graphs of the effects, graphs of the coefficients of variation) (Fig. 2).

Once the model is built, it is easy to let a parameter vary (either an operational parameter, an intrinsic, or a semi-empirical one [17]) according to the selected distribution laws and to observe the effects of these distributions on the electrical response of the cell. It is also straightforward to identify some semi-empirical parameters and to observe their effects on the electrical response. Multiple parameters variations are also possible.

Each analysis can be started from a particular state of the FC simulation (for instance, the nominal operating conditions of the cell) to analyze the impact of the parameter uncertainty on the distribution obtained on the model responses (Fig. 2). There are several classic statistic laws available in the DYMOLA software. In the nominal conditions and without considering degraded modes, the Random Normal Law is used to observe the electrical responses of the cell. For more complex cases (i.e. degraded modes), all the laws that have been mentioned previously can be applied specifically to match better with the representations of the different groups of parameters (physical parameters, operational parameters or semi-empirical coefficients used in the sub-models). In order to define some statistical distributions, 2000 (or even more) simulations can be run. Here, the reliability can be defined as the probability for the FC to deliver a minimal cell voltage (U_{min}) or a minimum of power (for a given load current). The sensitivity analysis allows linking this probability level to the variation rate of the parameter that has been considered as uncertain in the model.

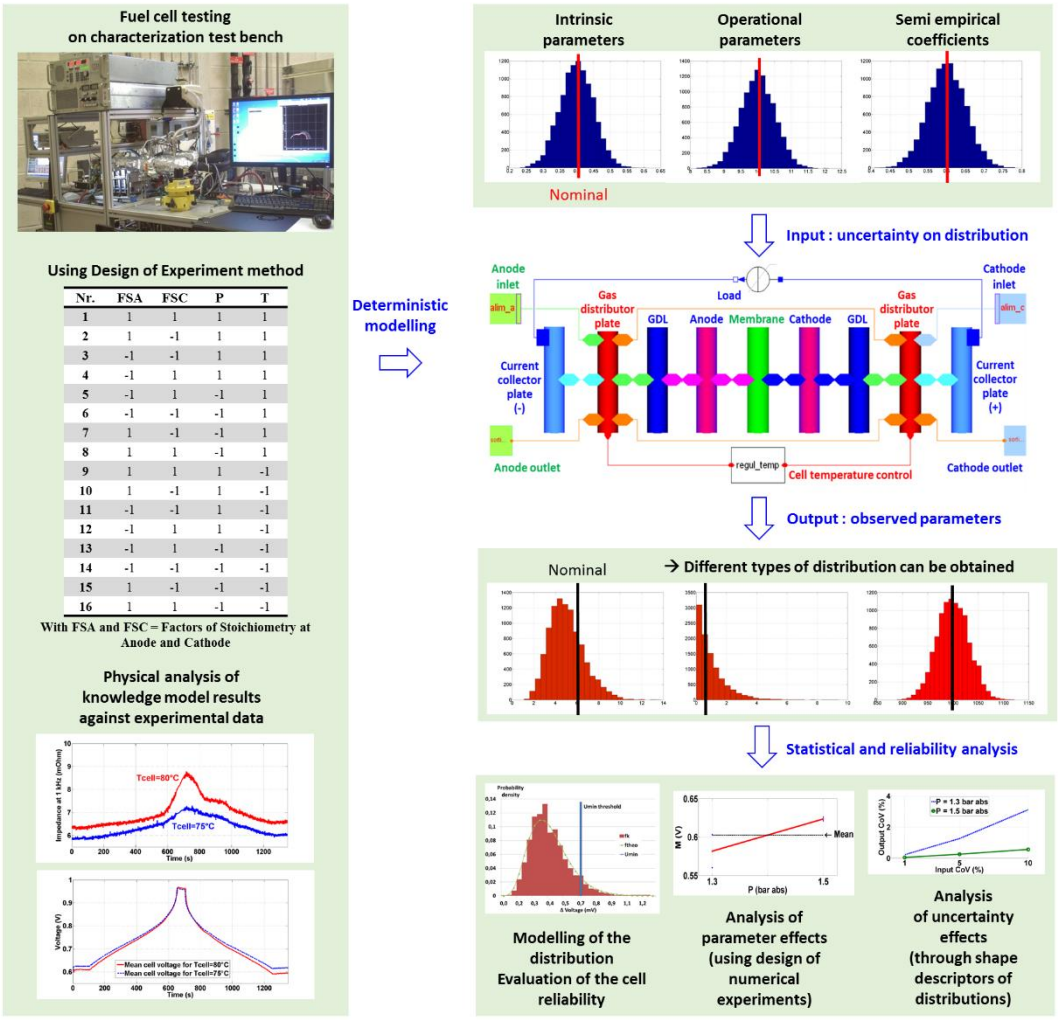

Nr.	FSA	FSC	P	T
1	1	1	1	1
2	1	-1	1	1
3	-1	-1	1	1
4	-1	1	1	1
5	-1	1	-1	1
6	-1	-1	-1	1
7	1	-1	-1	1
8	1	1	-1	1
9	1	1	1	-1
10	1	-1	1	-1
11	-1	-1	1	-1
12	-1	1	1	-1
13	-1	1	-1	-1
14	-1	-1	-1	-1
15	1	-1	-1	-1
16	1	1	-1	-1

Fig. 2. Schematic representation of the integration process and analysis of the uncertainties in the knowledge model developed under DYMOLA [17].

After describing the method for integrating one or more uncertainties in our FC model, we perform a statistical and reliability analysis of a response given by the model through an example of drawings.

4. An example of statistical and reliability analysis: the integration of uncertainty about the porosity of GDL

In this study, the uncertain parameter that we consider is the porosity of the GDL at the cathode side. The GDL porosity is an interesting geometrical parameter to investigate since it is closely linked with the possible physical mechanisms of degradation affecting the GDL layers. The durability research summaries focusing on GDL degradation are relatively limited, even though it might be a key-factor for managing mass transport and two-phase flow while mechanically supporting a MEA and a bipolar plate [29-31]. According to Jaeman Park et al. [31], GDL degradation can be categorized into mechanical (including the compression force effect, freeze/thaw cycle effect, dissolution effect, and erosion effect) and chemical degradation (which consists of the carbon corrosion effect). The effects of the GDL porosity on the PEMFC

performance can be described through well-suited modelling tools including transient transport processes with two-phase flow representations in the layers [16, 32, 33].

In our study, the uncertainty on the GDL porosity can be related with some imperfections in the manufacturing process and / or with some minor damages which only moderately affect the FC performance (i.e. no blocking of the reactants in the GDL, no perforations in the layer). The Gaussian (or Normal) distribution is then well-suited to represent this type of uncertainty; it is used to have a realistic behavior of the considered uncertainties. The Gaussian distribution is described by the following two pattern parameters: the nominal value of the variable (average *m)* and the percentage of the dispersion of the variable (coefficient of variation *CoV).* This one is defined as follows:

$$CoV = \sigma / m \tag{8}$$

where σ is the standard deviation of the variable.

4.1 Generation of statistical distributions on the input parameters

We consider a maximum dispersion (nor high nor low) equal to 10% [34]. To generate the statistical distribution of the GDL porosity at the cathode, 2000 values are drawn randomly. This number corresponds to a tradeoff between simulation duration and accuracy.
The characteristic shape of the input distribution is first observed, with the aim to ensure the Gaussian nature of the distribution. The values obtained for the descriptors of the distribution are compared with the reference values (Table 3). The algorithm that generates the distribution is re-run as many times as necessary.

Table 3. Characteristics of the input distribution (GDL porosity).

Parameters	Reference value	Value obtained
Mean value	0.6	0.6008
Standard deviation	0.06	0.0596
Coefficient of variation (%)	10	9.93
Peakedness (kurtosis)	3	3.1846
Asymmetry (skewness)	0	-0.1175

For the output distribution, the accuracy of the results is estimated using the method proposed by Mawardi et al. in [7]. It is briefly described below.
The quality of the statistical analysis is directly related to the accuracy obtained for the shape parameters describing the statistical distribution of the response. From a purely theoretical point of view, an infinite number of drawings is required to achieve stable average value and standard deviation. In practice, in order to limit the duration of the simulations, a limited number of drawings is selected and a convergence analysis of the output variable is performed. Figure 3 represents the average of the FC voltage as a function of the number of drawings used in the stochastic simulation. A convergence of the average value is observed for a little less than 2000 drawings.

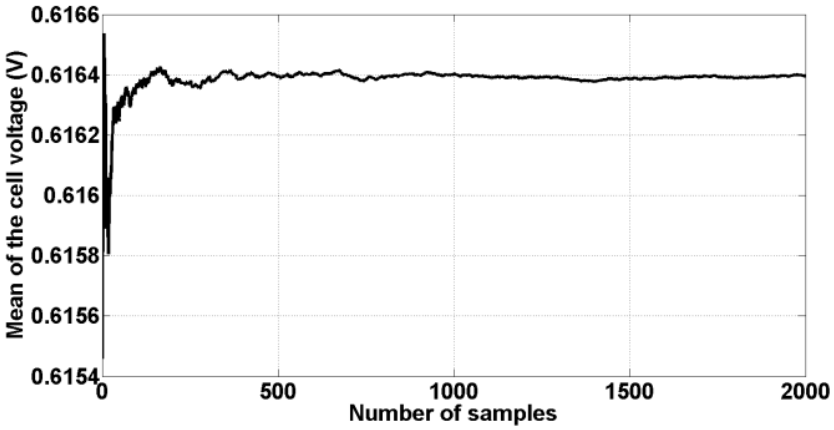

Fig. 3. Stochastic convergence analysis to determine the minimum number of samples / drawings required to obtain a stable cell voltage.

Each drawing corresponds to a temporal simulation conducted in 1000 seconds (the real computation time duration is between 1 and 2 seconds); this time interval allows obtaining a stabilization of the model variables. The real computation time required to perform the simulations from a series of 2000 drawings is between 33 and 66 minutes, depending on the integration step, the solver selected, and the desired accuracy. The characteristics of the computer used for the calculations are the following ones: Intel Xeon E5345 CPU @ 2.33 GHz, RAM: 12 GB.

The distributions obtained for the input parameter (porosity of GDL at the cathode) and for the response of the model (FC voltage) are shown in Fig. 4.

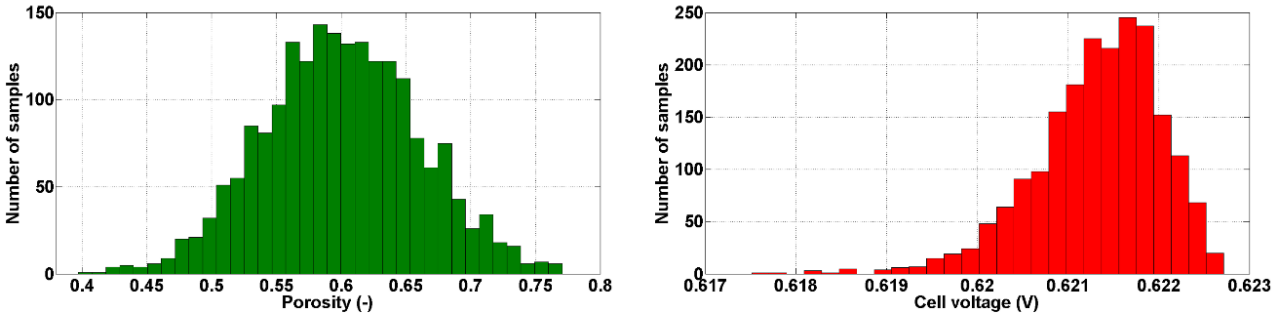

Fig. 4. Distributions obtained after 2000 drawings (cell simulations in nominal operating conditions).

- On the left side: for the input parameter, i.e. the porosity of the GDL (mean value = 0.6; *CoV*=10%).
- On the right side: for the response, i.e. the cell voltage.

By observing the shape of the response distribution obtained for an uncertainty of 10% on the porosity (Fig. 4. (right side)), a dispersion of a particular nature is detected. According to the theory of K. Pearson on the probability surfaces [35], this dispersion can be represented by a special statistical law named symmetric Gamma law.

- **"Simple" model vs. knowledge model confrontation**

It is possible to introduce some uncertainty in the equation of the "simple" model mentioned in Section 2 and corresponding to a steady-state FC voltage vs. current characteristics (Eq. (1)). For instance, the uncertainty can be applied to the semi-empirical β5 in Eq. (1). The results

obtained do not show any complex effects between the input and the output of the model (Fig. 5). In this case, a Gaussian distribution applied to an input parameter induces another Gaussian distribution type on the response. On the contrary, Fig. 4, related with the knowledge model, highlights the nonlinear nature of the modeled phenomena. The distribution of the responses (FC voltage) has not the same nature as the distribution applied to the input parameter (GDL porosity). Instead of a Gaussian distribution, a symmetric Gamma distribution is detected.

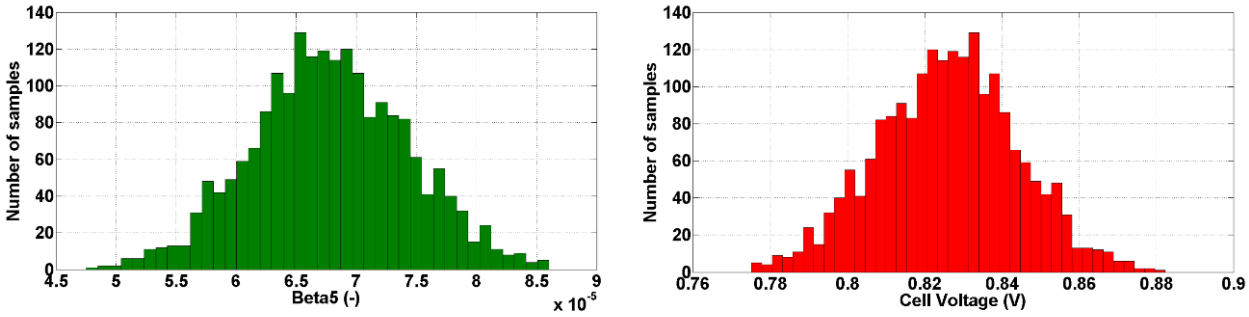

Fig. 5. Example of distributions on the semi-empirical $\beta 5$ input parameter (left) and the response (right) obtained when using the "simple" model only.

4.2 Physical interpretation for the shape of the output distribution

In this section, we provide the first explanations about the shape of the observed distribution. The comments provided are based on the adopted physical modeling. Further explanations will be given in Section 4.3.

Under the same FC operating conditions, we observe that the increase of the dispersion on the input (coefficient of variation ranging from 1% to 5%, then 10%) leads to an output distribution with a shape that gradually approximates an inverse Gamma law type (Fig. 6.). The increase of the GDL porosity facilitates the diffusion of the gas from the channel plate to the electrode. The pressure drop in the GDL is then reduced. The pressure of oxygen in the electrode becomes higher, which results in a higher cell voltage. However, this improvement of the electrical performance is limited by the passage of the reactant in the GDL (saturation of the flows through the pores of the layer) and / or in the electrode itself that also imposes a limit to the diffusion. This phenomenon of threshold, i.e. of gas diffusion limit, explains the upper limit that appears on the voltage. The change of shape affecting the distribution of the FC voltage (evolution towards a symmetric Gamma law) is physically linked to the limit imposed by the diffusion of the reactants in the MEA.

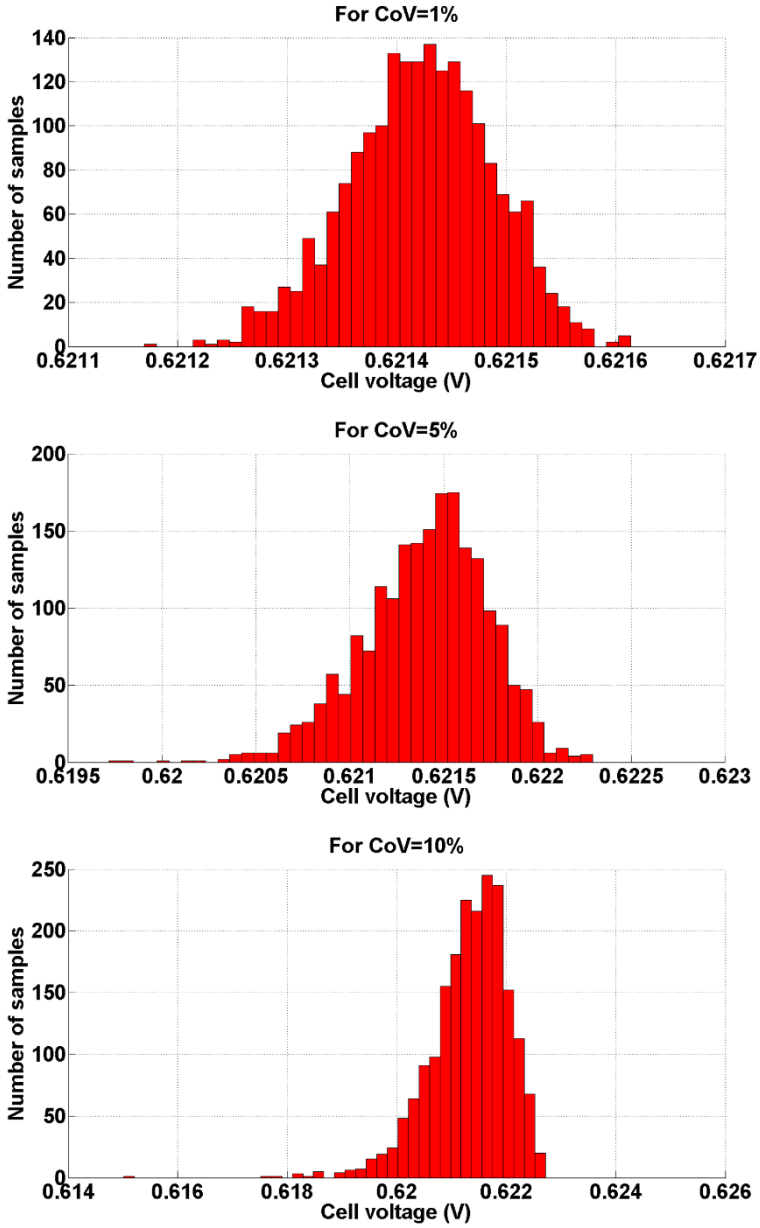

Fig. 6. Distribution of the cell voltage in the nominal conditions, for three input distributions:
- Coefficient of variation of 1% (top),
- Coefficient of variation of 5% (middle),
- Coefficient of variation of 10% (bottom).

4.3 Propagation of the uncertainties in the layers of the model

In this section, we show how the effect of an uncertainty introduced on a physical parameter (the porosity of the GDL) propagates inside the different layers of the modeled FC. We give a physical interpretation of how the propagation takes place, by referring to the knowledge model developed. The simulations are done in the nominal operating conditions.

As it is explained in Section 4.1, the dispersion of the porosity affects the FC voltage. This influence of the uncertainty on the voltage can be explained by the effect of the dispersion on the oxygen partial pressure in the electrode. We can observe that the distributions of oxygen partial pressure (Fig. 7 a)) and FC voltage (Fig. 6) have similar shapes. The increase of the diffusion layer porosity allows a better diffusion of the gases towards the catalyst layers, and

thus an increase of the partial pressure of oxygen at the electrode (Fig. 7 (top, left)). This increase of the oxygen pressure is partly limited by the electrode (having its own diffusion limit, as suggested in Section 4.2).
Compared with the other dispersions on oxygen and nitrogen partial pressures (respectively displayed in Fig. 7 (top, left) and (top, right)), the distribution obtained for the water vapor partial pressure shows a different shape. This can be explained by the fact that the steam is introduced at the cell inlet (for membrane humidification purpose) while it is also produced inside the MEA through the electrochemical reaction. Unlike water vapor, oxygen and nitrogen are only provided to the cathode, and not produced in the electrode. The changes of the water vapor partial pressure will then have some evolutions in opposition to the two other species. These different directions of change will induce some forms on the distributions that could be described as "complementary". In other words: at constant total pressure in the cathode, the steam produced will occupy the space left vacant by the two other gases. When oxygen and nitrogen diffuse worse through the GDL (from the bipolar plate to the electrode), they leave more free space for the water vapor (so, at constant total pressure, the partial pressure of the water vapor will increase).
The value of the vapor partial pressure is also limited by the vapor saturation pressure: once this value is exceeded, a portion of the water vapor condenses to form liquid water. In Fig. 7 (bottom, left), we can observe that the distribution of the water vapor partial pressure has the form of a Gamma law.
As for the total pressure, it varies very little, of a few tens of Pascal (Fig. 7 (bottom, right)). The form of the distribution observed for this pressure seems to be similar to the dispersions obtained for the oxygen and nitrogen pressures.

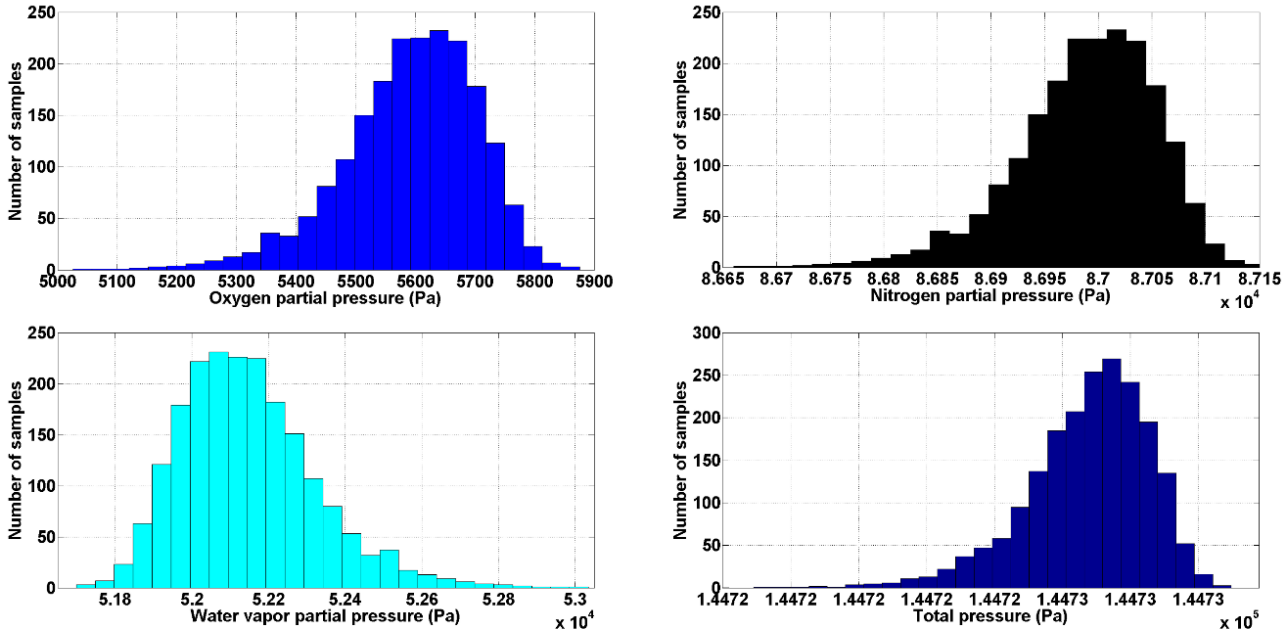

Fig. 7. Pressure dispersions in the electrode at the cathode side.
- Partial pressure of oxygen (top, left).
- Nitrogen partial pressure (top, right).
- Partial pressure of water vapor (bottom, left).
- Total pressure (bottom, right).

The partial pressures in the GDL (Fig. 8) seem to have a behavior similar to that of the pressures in the electrodes, except the total pressure (Fig. 8 (bottom, right)) that tends to follow a statistical law similar to that of the pressure partial vapor (Fig. 8 (bottom, left)). We observe

that the mean of the oxygen partial pressure (Fig. 8 (top, left)) is much higher in the diffusion layer than in the electrode. The nitrogen partial pressures in the electrode and in the GDL have the same order of magnitude (Fig. 8 (top, right)).

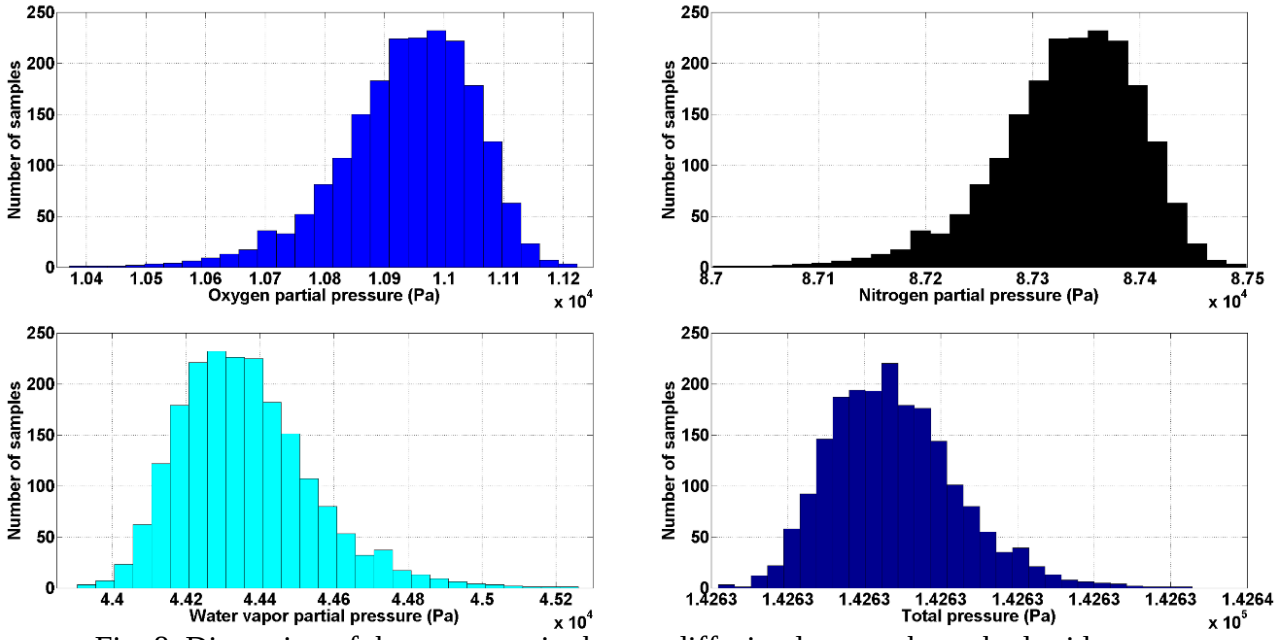

Fig. 8. Dispersion of the pressures in the gas diffusion layer at the cathode side.
- Partial pressure of oxygen (top, left).
- Nitrogen partial pressure (top, right).
- Partial pressure of water vapor (bottom, left).
- Total pressure (bottom, right).

In the following Section, the method used to integrate the uncertainties in the developed knowledge model is applied by implementing a design of numerical experiments related with different operating conditions.

5. Impact of input parameters on the cell performance variability

The objective of the study described in this section is to determine the impact of different GDL porosity dispersions on the FC performance (i.e. voltage and resistance of the cell) determined in different operating conditions. This study is conducted by implementing a numerical experimental design leading to a set of simulations conducted with the deterministic, knowledge model presented in Section 2.
We present in the following subsection the experimental design chosen.

5.1. Analysis conducted through a design of numerical experiments

We follow the steps of the experimental design approach [36, 37] to complete our study.
The factors considered are:

- the temperature T of the cell (average of the temperatures calculated in the reactant distribution plate) with two levels,
- the pressure P in the stack (total pressures of the reactants calculated and regulated at the stack inlets) with two levels,

- the coefficients of variation *CoV* for the uncertainty on the porosity of the diffusion layer at cathode side, with three levels,
- the FC load current *I* with 4 levels.

The levels of the factors are shown in Table 4.

Table 4. Levels of the factors considered in the design of experiment.

	Factors				
Temperature [° C]	*T*	75	80		
Pressure [bar abs.]	*P*	1.3	1.5		
Coefficient of variation for the porosity [-]	*CoV*	1	5	10	
Current [A]	*I*	70	110	150	170

The operating parameter range (*T*, *P*, *I*) is defined in order to explore a significant "experimental domain" (as wide as possible, according to the Design of Experiment - DoE method) around the nominal FC operating point, while maintaining relatively homogeneous behaviors for the cells in the stack. In fact, this "experimental domain" could potentially allow an optimization (e.g. with respect to the reliability rate as it is defined in [17, 18]) of the nominal operating conditions, that were initially defined by the FC manufacturer both for a new PEMFC (i.e. at the beginning of its life) and for a stack including a higher number of cells (i.e. designed for automotive applications). The choice of two levels for the factors *T* and *P* implies that we assume some linear variations of the phenomena between these two states. The parameter levels are also set so that they are not too close from each other (to be able to distinguish the effects of the two levels on the response). It is also necessary that the levels are not too far from each other so that the linearity assumption remains realistic.

We use a factorial design [36, 37] to perform the experiments (total number of experiments: 48); each experience leads to 2000 drawings, i.e. time domain simulations (for the full design related with one current level, the real computing time is about 24 hours). The experimental design for a single current level is given in Table 5.

Table 5. Design of Experiments for a load current of 110 A.

No.	*T*	*P*	*Co V*	*I*
1	75	1.3	1	110
2	80	1.3	1	110
3	75	1.5	1	110
4	80	1.5	1	110
5	75	1.3	5	110
6	80	1.3	5	110
7	75	1.5	5	110
8	80	1.5	5	110
9	75	1.3	10	110
10	80	1.3	10	110
11	75	1.5	10	110
12	80	1.5	10	110

The studied responses are the battery voltage and the membrane resistance. The parameters that can be observed correspond to the shape descriptors of the output distributions: the mean, standard deviation, kurtosis, asymmetry and shape parameters specific to the Gamma distribution *(a* and *p).*

The study can be conducted using different tools linked with the design of experiments method: graphs of effects and interactions, and ANOVA tables [36, 37]. Numerous articles related with works conducted in the PEMFC research area and using design of experiments techniques and/or ANOVA can now be found in the literature [38].
In [38], Wahdame et al. propose a review of various design of experiments applications in the field of FC research. Some examples of works are detailed. A conceptual typology of different possibilities offered by the design of experiments methodology in the FC domain is also given. More recently, in [39], Goulet et al. use a factorial study and some ANOVAs to quantify the effects (and their statistical significance) of the humidity and temperature parameters on the mechanical properties (modulus, yield stress) of both a pure perfluorosulfonic acid membrane and a Catalyst Coated Membrane (CCM). The final results of this work emphasize the importance of the catalyst layers on the overall mechanical properties of the CCM. The authors demonstrate that catalyst layers contribute to the mechanical reinforcement of the membrane and also increase the contraction forces due to dehydration. In [40], Khorasany et al. develop an ex-situ tensile fatigue experiment to explore the mechanical stability of FC membranes under a range of controlled environmental conditions. A statistical design of experiments approach is applied to determine the effects of temperature and relative humidity on the maximum stress and final strain at rupture. In the study, the effect of temperature is found to be more significant, with reduced fatigue life at high temperatures. Some ANOVA results confirm the statistical significance of the work findings and further demonstrate a counteracting interaction effect of temperature and humidity.

In the next Section, we mainly take advantage of the graphs of effects and interactions to study the impact of the factors (operating conditions and dispersion of porosity) on the responses (cell voltage). We also use some ANOVA tables as complementary tools in particular to determine the statistical significance of the factors on the responses.

5.2. Effects of the factors on the cell voltage. A graphical analysis

For various cell currents, we study the effects of factors *(T, P, CoV)* and interactions between two factors *(P * T, CoV * T, CoV * P)* on two shape parameters (mean *M* and standard deviation *E)* of the statistical distribution of the voltage responses obtained with the model developed. This study is conducted by displaying the graphs of effects and interactions (Table 6). On these graphs, the slope of the lines indicates the magnitude and direction of the effects, whereas the lack of interaction effect is represented by a parallelism of the lines. The study is supplemented by giving the related ANOVA tables (Tables 7 and 8) [36-38].

Regarding the graphs of the effects related with the mean *M* (left column of Table 6), the following observations can be made:

- The temperature *T* has a negative effect on the mean of the voltage distribution; an increase in cell temperature from 75 to 80°C lead to a significant decline in FC performance (about -20 mV on the cell voltage).
  The "simple" model mentioned in Section 2 was also used in [18] to analyze the effect of temperature on the electrical performance. An opposite effect was detected; an increase in performance was observed for the highest temperature level. This was due to the decrease in the activation overvoltages of the current - voltage law used in the "simple" model; the electrolyte resistance had a constant value that was not affected by the temperature. In the model of knowledge, the temperature parameter plays various roles in many sub-models / cell layers. For instance, the temperature has an influence

on the activation overvoltage but also on the hydration of the membrane, and thus on its resistance.

The model of knowledge allows us to find some cell behaviors and some effects of temperature similar to those observed in the experiments described in [18] - Chapter 1.

- An increase in the pressure *P* has a positive effect on the mean of the voltage distribution; an increase in pressure from 1.3 to 1.5 bar abs. generates a gain of about forty mV on the cell voltage. This result was expected; it was already found during the tests and analysis of the parameter effects conducted on the basis of the "simple" model [18]. Increasing the pressure decreases the activation overvoltage and results in an increase of the overall cell voltage. In the knowledge model, as well as with the experimented FC [18], the pressure plays a role in the water exchanges. We will see in the analysis of the effects based on the average of the distribution of the membrane resistance that higher pressure promotes the hydration of the electrolyte (Section 5.5).
- In comparison with other parameters, a change of the dispersion on the GDL porosity at the cathode has very little effect on the average value of the voltage distribution. This seems logical since the chosen input dispersions generate only very low dispersions on the output voltage distribution (standard deviation in the order of magnitude close to 0.1 to 1 mV).
- The *P* * *T* interaction is the most significant one. The knowledge model involves many mathematical expressions in which *T* and *P* parameters appear together (e.g. ideal gas law, equation of the saturated vapor pressure, diffusion laws of Stephan-Maxwell and Knudsen, etc.).

  In the analysis of the experimental tests conducted in [18] – Chapter 1, we could detect a slight impact of the *P* * *T* interaction on the cell performance. The knowledge model allows finding the presence and direction of this interaction. We find the effects of the above described parameters when we consider in turn their low and high levels.
- The ANOVA of Table 7 shows that only the *T, P, CoV* factors and the *T* * *P* interaction could be considered statistically significant ([18] - Appendix).

Regarding the graphs of the effects related to the standard deviation *E* (right column of Table 6), the following comments can be made:

- In the variation domain considered in this study, the *T* and *P* factors do not affect the standard deviation of the voltage distribution. These operating parameters have low and high levels that are constant (no dispersions introduced on the inputs related with *T* and *P);* therefore, they do not alter the shape of the distribution applied to the input of the model. Similar observations could be done in the analysis of the effects achieved on the basis of the "simple" model ([18] – Chapter 2).
- The dispersion introduced on the porosity parameter can be retrieved on the output voltage distribution. An ANOVA could show that this effect was significant from a statistical point of view ([18] - Appendix). An increase of the dispersion on the porosity causes an increase in the standard deviation of the output distribution (voltage). On the output distributions, we are not far from finding the variations of the coefficients introduced on the porosity (1%, 5% and 10%).
- The interactions *P* * *T, T* * *V,* and *V* * *P* were not found to be significant from a statistical point of view (Table 8). Also, it is difficult to give an explanation about the nature of these interactions.

Overall, at 110 A, Table 6 suggests that the parameters that lead to a higher average value also result in a reduction of the standard deviation value.

Table 6. The effects and interactions of the parameters *T*, *P*, and *CoV* on the voltage at 110 A.

	On the mean (V) of the distribution	On the standard deviation (V) of the distribution
T	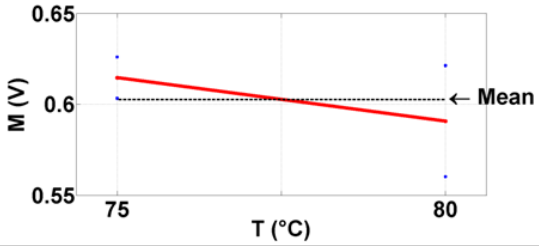	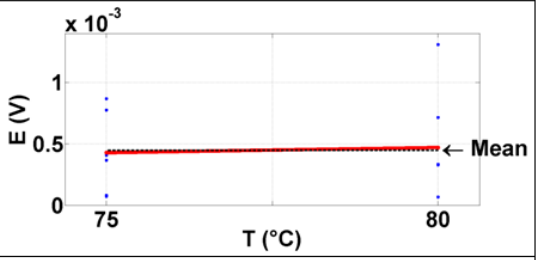
P	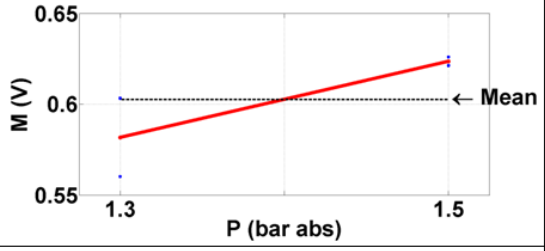	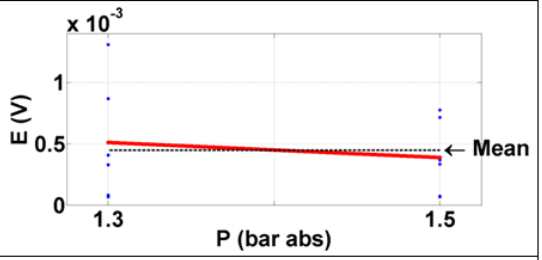
CoV	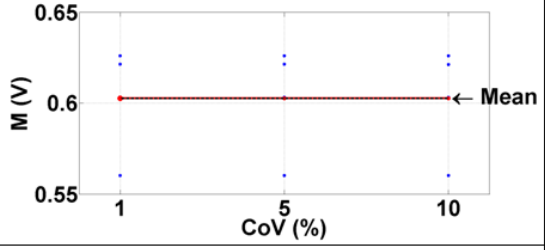	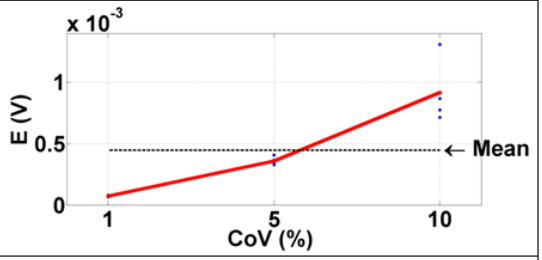
P* T	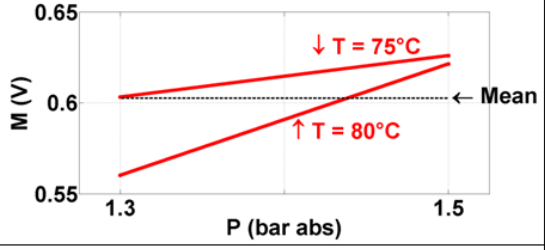	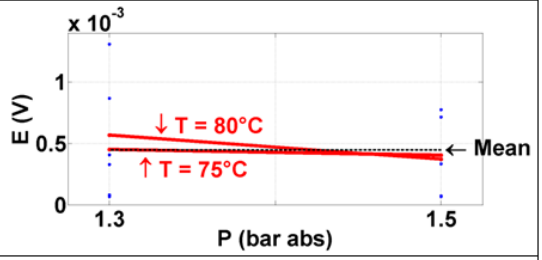
CoV* T	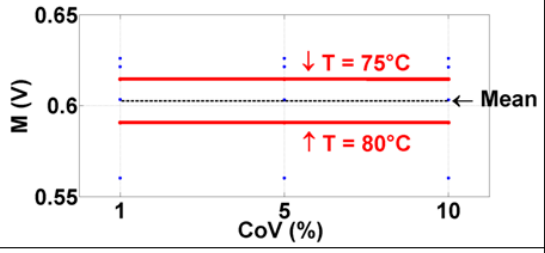	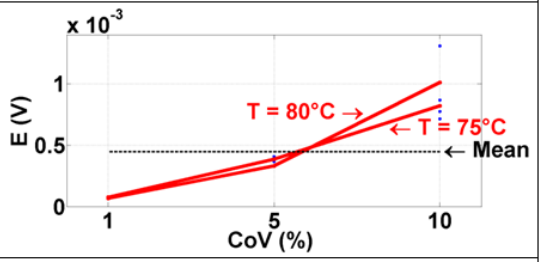
CoV* P	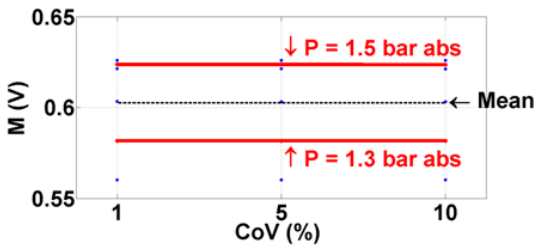	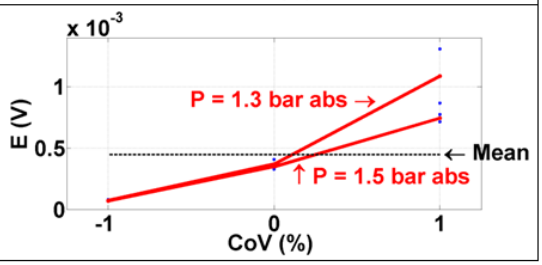

Table 7. ANOVA table computed at 110 A in nominal conditions, with *T*, *P*, *CoV* as input factors and with the mean voltage value of the distribution (*M*) as the response.

Source	*T*	*P*	*CoV*	*T* * *CoV*	*P* * *CoV*	*T* * *P*	Error
Sum sq.	1.71E-03	5.29E-03	1.00E-08	3.77E-09	2.52E-09	1.11E-03	3.74E-09
%	**21.1**	**65.2**	**0**	**0**	**0**	**13.7**	**0**
d. f.	1	1	2	2	2	1	2
Mean sq.	1.71E-03	5.29E-03	5.00E-09	1.89E-09	1.26E-09	1.11E-03	1.87E-09
fs	9.14E+05	2.83E+06	2.67E+00	1.01E+00	6.74E-01	5.94E+05	
fs_{theo}	8.5	8.5	9	9	9	8.5	
p-Value	0.9999989	0.9999996	0.7278020	0.5019973	0.4025559	0.9999983	
Test	**OK**	**OK**	**NO**	**NO**	**NO**	**OK**	

Table 8. ANOVA table computed at 110 A in nominal conditions, with *T*, *P*, *CoV* as input factors and with the standard deviation of the voltage distribution (*E*) as the response.

Source	*T*	*P*	*CoV*	*T* * *CoV*	*P* * *CoV*	*T* * *P*	Error
Sum sq.	5.25E-09	4.51E-08	1.48E-06	3.44E-08	7.38E-08	1.67E-08	4.68E-08
%	**0.3**	**2.6**	**87**	**2**	**4.3**	**1**	**2.8**
d. f.	1	1	2	2	2	1	2
Mean sq.	5.25E-09	4.51E-08	7.40E-07	1.72E-08	3.69E-08	1.67E-08	2.34E-08
fs	2.24E-01	1.93E+00	3.16E+01	7.35E-01	1.58E+00	7.14E-01	
fs_{theo}	8.5	8.5	9	9	9	8.5	
p-Value	0.3175918	0.7005361	0.9693477	0.4236453	0.6119403	0.5128276	
Test	**NO**	**NO**	**OK**	**NO**	**NO**	**NO**	

5.3. An example of polynomial / statistical model of the voltage response as a function of the parameters studied

Once the calculations of the effects and interactions are made, it is possible to propose a statistical, polynomial model of the responses obtained in the experimental design presented above. We will give the equation of such a model in the case of the mean FC voltage M_{UFC} (computed at 110 A). The three parameters that have the largest influence on the average voltage (i.e. *T*, *P*, and *P* * *T*)) will be considered in this modeling. The model will have the following form:

$$\begin{aligned} M_{UFC} = \quad & M + \begin{bmatrix} E_{T_{(-1)}} & E_{T_{(+1)}} \end{bmatrix} \cdot [T] + \begin{bmatrix} E_{P_{(-1)}} & E_{P_{(+1)}} \end{bmatrix} \cdot [P] \\ & + \begin{bmatrix} E_{CoV_{(-1)}} & E_{CoV_{(0)}} & E_{CoV_{(+1)}} \end{bmatrix} \cdot [CoV] \\ & + [T]^t \cdot \begin{bmatrix} I_{T_{(-1)}P_{(-1)}} & I_{T_{(-1)}P_{(+1)}} \\ I_{T_{(+1)}P_{(-1)}} & I_{T_{(+1)}P_{(+1)}} \end{bmatrix} \cdot [P] \end{aligned} \tag{9}$$

$$M_{UFC} = \quad 0.603 + [1.19 \cdot 10^{-2} \quad -1.19 \cdot 10^{-2}] \cdot [T] + \; [-2.1 \cdot 10^{-2} \quad 2.1 \cdot 10^{-2}] \cdot [P]$$
$$+ [3 \cdot 10^{-5} \quad 9.1 \cdot 10^{-6} \quad -3.91 \cdot 10^{-5}] \cdot [CoV] \qquad (10)$$
$$+ [T]^t \cdot \begin{bmatrix} 9.62 \cdot 10^{-3} & -9.62 \cdot 10^{-3} \\ -9.62 \cdot 10^{-3} & 9.62 \cdot 10^{-3} \end{bmatrix} \cdot [P]$$

It is possible to achieve the same type of modeling for the other shape parameters studied (e.g. standard deviation of the distribution) and the other output parameters, such as the membrane resistance. The generated models allow simple and synthetic representations of the results obtained after several hours of computing done with the knowledge model. Then, such polynomial models could be easily implemented in further reliability studies.

5.4. Graphs of the coefficients of variation (Mawardi and al. [7])

To complete this graphical analysis of the effects of factors on the FC voltage, we consider the output distributions descriptors and their trends depending on operating parameters. As an example, we study the evolution of the coefficient of variation related with the output (i.e. *CoV* of the output = *CoV* of the voltage distribution) distribution vs. the FC current, and for different coefficients of variation introduced into the input distribution linked with the GDL porosity at cathode (*CoV* of the input). For the record, the coefficient of variation is the ratio of the standard deviation to the arithmetic mean.

In Fig. 9, we observe that the output dispersion increases with the current, initially relatively slowly between 70 and 150 A, then increases from 150 to 170 A for the three *CoV* considered as inputs. Whatever the cell current value, an increase in the dispersion of the porosity leads to a larger dispersion of the voltage response. We had already noted in the comments of Table 6, linked to the Figure showing the standard deviation as a function of the input *CoV* that the dispersion introduced on the porosity parameter could be retrieved on the output (voltage) distribution. We can also note in Fig. 9 that the ratio between two levels of input *CoV* is equal to the ratio between the two output *CoV*. For example, at 110 A, for inlet *CoV* values equal to 1 and 5%, we have some output *CoV* respectively equal to 0.011 and 0.059%, that means a ration close to 5 between these two values.

Some physical explanations can be provided about the shape of the curves shown in Fig. 9. When the cell current increases, the oxygen consumption in the electrode becomes stronger. The oxygen flow through the GDL also increases. Some variations on the porosity of the GDL will result in a partial pressure variation of oxygen at the electrode and thus, in a dispersion of the electric potential at cathode. Therefore, the higher the variation of the GDL porosity, the larger is the variation of the voltage. It is also likely that the increase of the current (which leads to an increase of the oxygen flow in the GDL) amplifies, at the electrode, the effect of the porosity dispersion on the oxygen pressure, and thus on the cathode voltage.

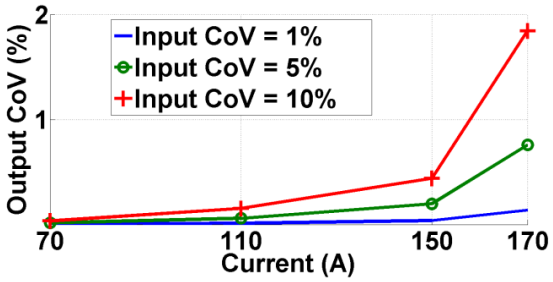

Fig. 9. Evolution of the coefficient of variation for the output (Output *CoV*) versus the FC current, and as a function of the dispersion on the porosity (Input *CoV*).

This type of figure leads us to use some graphs such as those proposed by Mawardi et al. [7] representing the coefficients of variation of the responses vs. the coefficients of variation of the input parameters. We show in Table 9 some graphs of the output coefficients of variation (voltage) vs. input coefficients of variation (GDL porosity), for different levels of FC operating parameters (*T*, *P*, and *I*).
This type of graphical representation corresponds to an alternative way to the graphs of the effects for the study of the impacts of the porosity variation on the voltage dispersion. In fact, through these new graphs and the output *CoV*, we observe a combination of the responses observed in Table 9 (mean and standard deviation). Furthermore, in Table 9, the analysis can be made for different current levels.
Thus, in Table 9 at 110 A, the figure related to the temperature is very similar to that of the effect of the *CoV* * *T* interaction on the standard deviation in Table 6.
Table 9 can be utilized to determine the operating parameters *T* and *P* leading to the lowest *CoV* output (highest average values and lowest standard deviation values). For example, at 110 A, a pressure of 1.5 bar abs. leads to a lower *CoV* for the voltage.

These findings can be related with the observations made by Weber et al. in [16] (in the Section entitled "Modeling Stochastic and Statistical Performance" of their article) on the basis of the example devoted to the study of a GDL thickness variation determined by statistical parameters, and of its effects on the cell polarization curve characteristics. From the available current – voltage plots, the authors note several interesting aspects.
First, the statistical variation of the experiment widens as the load current increases; the cell becomes gradually sensitive to various aspects of the material properties or manufacturing variations. Weber et al. indicate that stricter tolerances or controls on the GDL properties may be required depending on the desired cell operating point.
Second, the authors notice that some combinations of material characteristics result in the formation of a characteristic "performance knee" in the 1.2 to 1.4 A/cm2 region of the polarization curve, where other combinations do not lead to such a behavior. As mentioned by Weber et al., considering the inputs, this aspect seems to be at least in part derived from multiphase flow phenomena.
In the summary of their study and article section, Weber et al. suggest that the statistical nature of the GDL materials, as well as the statistical nature of the performance data itself, should lead to the use of a statistical basis for the investigation of the information derived from performance or durability simulations conducted in this field.

Table 9. Coefficient of variation for the output (voltage) versus the coefficient of variation for the input (GDL porosity). For different levels of operating parameters (*T*, *P*, and *I*).

	Temperature	Pressure
70A	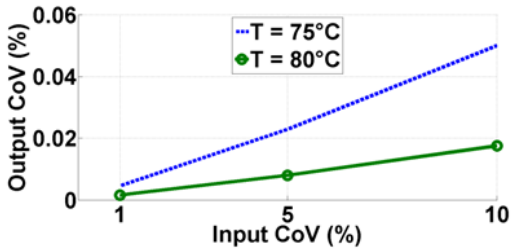	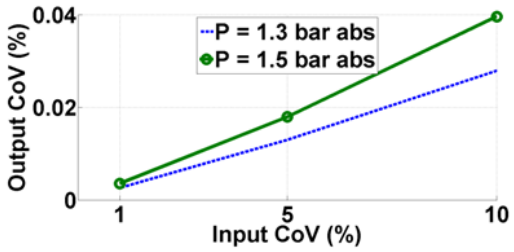
110A	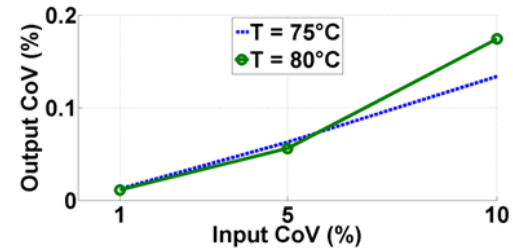	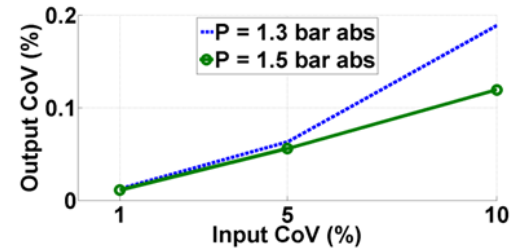
150A	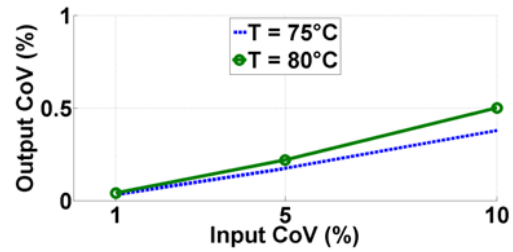	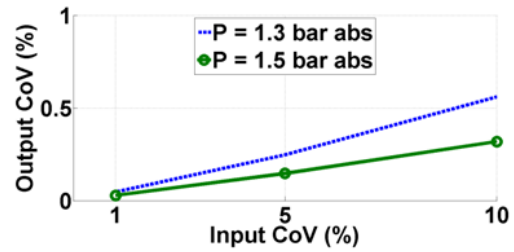
170A	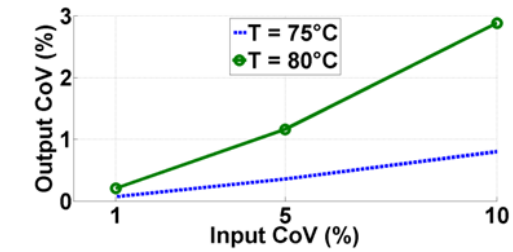	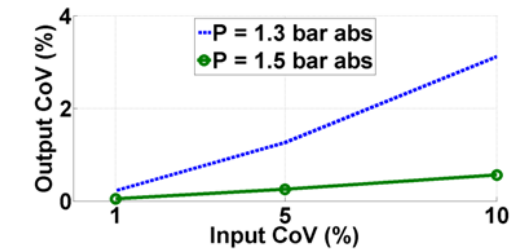

In the next section, a similar study is conducted to determine the impact of input factors (operating conditions, and dispersion on the porosity) on the response related to the membrane resistance.

5.5. Graphical analysis of the effects of factors on the cell membrane resistance

The observation of the effect of the Gaussian input distributions (porosity) (Fig. 10 (left)) on the membrane resistance highlights some behaviors similar to those observed for the dispersions of the cell voltage. Indeed, the output distributions of the resistance also correspond to symmetric Gamma type laws (Fig. 10 (right)).

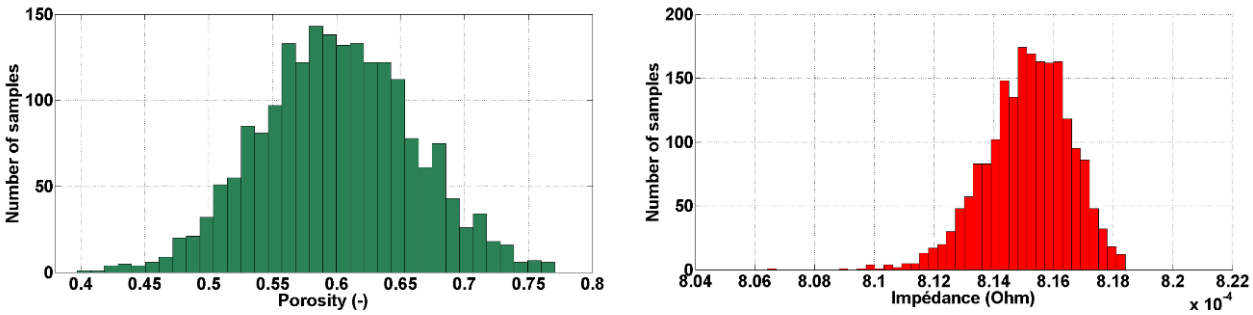

Fig. 10. Distributions obtained after 2000 drawings (cell simulations in nominal operating conditions).

- On the left side: on the input parameter, the porosity of the GDL at cathode (mean value = 0.6; *CoV*=10%).
- On the right side: on the response, here the membrane resistance.

For various cell current levels, we study the effects of factors (*T*, *P*, *CoV*) and interactions between two factors (*T* * *P*, *CoV* * *T*, *CoV* * *P*) on two shape descriptors (the average *M* and the Standard Deviation *E*) of the statistical distribution related to the membrane resistance calculated by the model developed. This study is conducted from the graphs of the effects and interactions (Table 10).

Regarding the graphs of the effects for the average *M* (left column of Table 10), the following observations can be made:

- The temperature *T* has an effect on the mean of the distribution of the resistance: an increase in the cell temperature from 75 to 80°C results in a significant reduction of the FC performance.
  Obviously, the "simple" model described in Section 2 does not allow such an analysis as in this case, the resistance of the membrane is modeled by a constant value. The knowledge model, in turn, allows finding some behaviors of the stack and effects of temperature similar to those observed in the experimental tests described in [18] - Chapter 1.
- An increase of the pressure *P* has an effect on the mean of the resistance distribution: an increase in pressure from 1.3 to 1.5 bar abs. generates a reduced resistance on the order of 0.2 mOhm. This result makes sense from a physical point of view; it had already been found during testing. The increase in the total pressure retains some moisture in the stack, which promotes the hydration of the electrolyte.
- Compared with other parameters, a change of dispersion on the GDL porosity at the cathode has no effect on the mean of the distribution of resistance. There were neither effects on the average of the voltage.
- The interaction *P* * *T* is the most significant one. It is noted that in the model results, for a pressure of 1.5 bar abs. (high level for *P*), the temperature has no influence on the resistance. At higher pressure, the membrane remains hydrated whatever the temperature (75 or 80°C). In the tests described in [18] - Chapter 1, the temperature had a slight effect on the resistance even at 1.5 bar abs.

Regarding the graphs of the effects related to the standard deviation *E* (right column of Table 10), the following observations can be made:

- In the domain of study considered, the factors *T* and *P* have a slight impact on the standard deviation of the resistance distribution. The effects vary in the same direction as those observed on the average: a higher average resistance corresponds to a resistance with a more unsteady value.

- As for the distribution of the voltage, the dispersion introduced on the porosity parameter is detected on the output distribution of resistance. An ANOVA could show that this effect was significant from a statistical point of view ([18] - Appendix). An increase of the dispersion on the porosity causes an increase in the standard deviation of the output distribution (resistance).
- The interactions *P * T*, *T * V*, and *V * P* are not significant from a statistical point of view ([18] - Appendix).

Overall, at 110 A, Table 10 shows that the levels of the parameters *T* and *P*, which lead to a decrease in the average resistance, also cause a drop in the standard deviation.

Table 10. Table of the effects and interactions of the parameters on the resistance at 110 A.

	On the mean (V) of the distribution	On the standard deviation (V) of the distribution
T	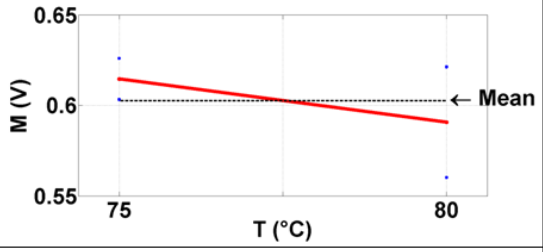	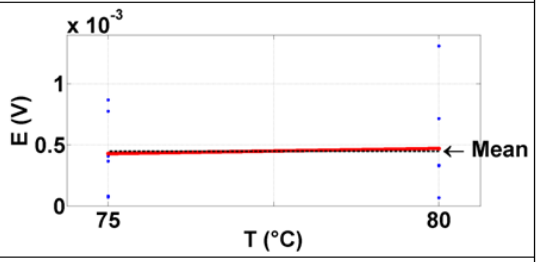
P	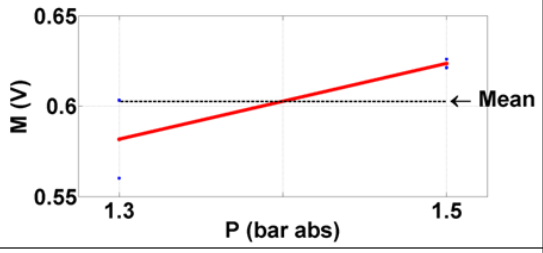	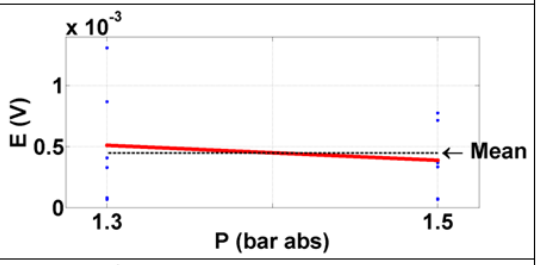
CoV	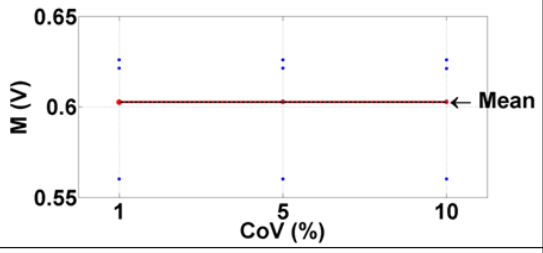	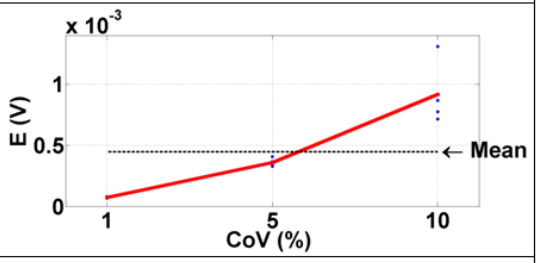
P* T	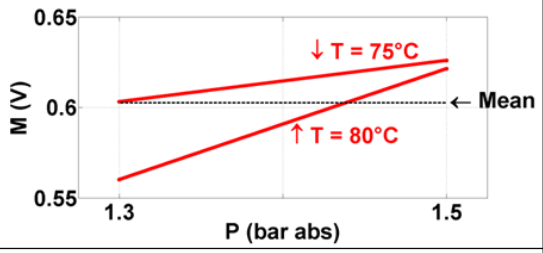	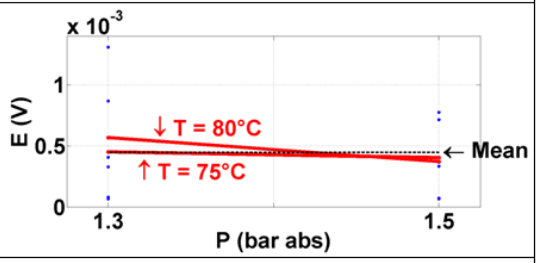
CoV* T	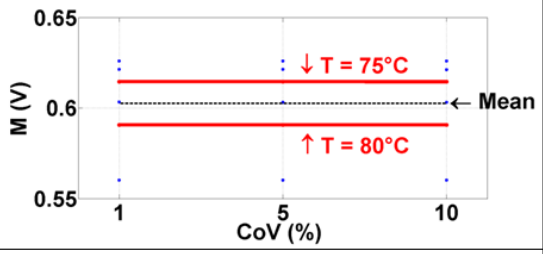	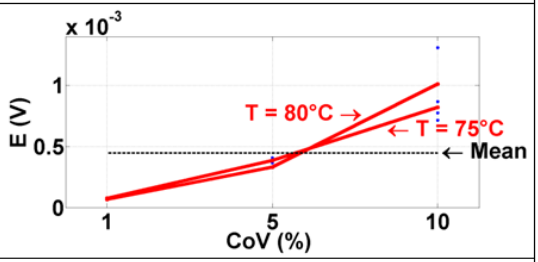
CoV* P	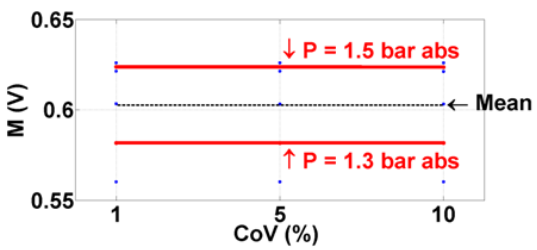	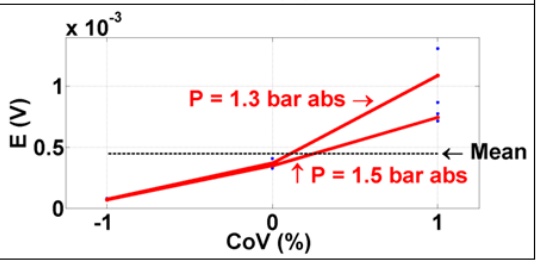

6. Conclusion

The knowledge / deterministic model, presented in Section 2, was used in the frame of the methodology presented in Section 3, and dedicated to the integration and analysis of uncertainties in a PEMFC modeling tool.
After a reminder about the general approach adopted, we have indicated differences that could be observed in the simulation results obtained from both types of modeling ("simple" and knowledge model): in the knowledge model, a Gaussian distribution of a parameter input as the GDL porosity may result in a distribution in response (cell voltage or membrane resistance) with a more complex shape (symmetric Gamma type for example). The difference between the shapes of the input and output distributions is the expression of strong nonlinearities and complexities linked with the phenomena considered in the knowledge model.

An example of statistical and reliability analysis is presented in Section 4 of the article. As an example, we chose a variation of the GDL porosity at the cathode as an uncertainty to be introduced into the knowledge model. In our view, the GDL porosity is an interesting geometrical / mechanical parameter to investigate since it can be a possible link between the fluidic sub-models already included in the tool and the mechanical sub-models that we would like to integrate to the knowledge model, in future stages of the model development. In particular, some recent results obtained from ex-situ mechanical – electrical characterization tests of GDL should be considered in this aim [27, 28].

In Section 4, we have detailed the input distribution generation method by including the number of drawings (2000) required to obtain results allowing a convergence of the output variable (voltage and resistance), the simulation time (1000 s simulated) required to achieve a stable output, the overall computation time for a series of 2000 drawings (between 33 and 66 minutes). We sought to provide a physical explanation for the observed shape of the output distribution: an inverse Gamma distribution with a threshold phenomenon on the voltage that was linked with a diffusion limit of the reactant in the MEA. The spread in the model of the influence of the uncertainty introduced was also observed and discussed. On this basis, in [17, 18], we could propose an output distribution modeling and introduce the reliability as the probability that the cell provides a minimum voltage U_{min}. An example of calculation for determining this probability in conditions of cell usage can be found in [17]. Under nominal conditions, the estimated level of reliability (likelihood that the model of the cell provides a minimum voltage of 0.68 V) was estimated at 91% with an input coefficient of variation of 10%.

In the last Section of the paper, the introduction of the uncertainties in the knowledge model method was applied by implementing a design of numerical experiments to study the impact of the uncertainty (still related with the GDL porosity at cathode) on the FC performance under different operating conditions. To this aim, we followed the steps of the experimental design approach [36, 37] to complete our study. All 48 distributions related on the one hand to the cell voltage and on the other hand to its resistance were analyzed using some graphs of the effects and some charts comparing the coefficients of variation of the input and output distributions (charts proposed by Mawardi et al. in their work on PEMFC [7]). The graphs of the effects were confronted to other graphs available in [18], related with experimental tests and simulation results obtained from the "simple" modeling. The graphs of the effects displayed from the simulation results obtained with the knowledge model (and the associated polynomial models) allow finding the influences of operating parameters (T and P) on the cell voltage and resistance. They attest to the inclusion in the modeling of complex phenomena related to the water and the

different gas species management. We also found that the variation coefficient related to the GDL porosity of the cathode had, compared to the other parameters considered and in the intervals of variation considered, little effect on the average output distributions. However, the dispersion introduced on the porosity had some impacts on their shapes (significant effect on the standard deviation).

For different levels of cell current, the design of numerical experiences achieved allows determining the levels of operating parameters (here the temperature and pressure) which limit the impact of the input uncertainty (GDL porosity) on the studied response (voltage or cell resistance). In the same vein, it would be possible to determine each of the projected reliability rates (relating to the same minimum threshold voltage) for the different cases of the design of numerical experiments and to conduct an optimization: to search the input parameters of the design leading to the highest level of reliability.

It would also be possible to address the problem of the GDL aging by choosing a degradation law for this component like in the work of Placca et al. [9, 10]. This could be done for example by indexing the coefficient of variation of the porosity on the FC operating time. The results we obtained could be utilized to select varying operating parameters over time, likely to minimize the dispersion in the response and to maintain high reliability rates. This shows that our model and our approach could be part of a broader framework of predictive maintenance.

The knowledge model developed and the approach recommended to integrate, analyze uncertainties in FC modeling could also be used for future works:

- Consideration of stoichiometric factors at anode and cathode in the numerical design of experiments presented Section 5.
- Introduction of uncertainties on other types of parameters (operating or semi-empirical ones). Observation of other answers (e.g. temperatures).
- Using other statistical tools for the analysis of results (e.g. Signal-to-Noise Ratio - SNR).
- Introduction of different types of statistical distributions on the model inputs.
- Using other shape descriptors for the analysis of distribution (skewness, kurtosis, ...).
- Simultaneous introduction of several uncertainties.
- Implementation of fractional designs of experiments to reduce the overall computation time associated with the simulations of drawings.

As already mentioned, in future works related with the development of the knowledge model, it will be possible to implement some additional physical phenomena such as the mechanical ones that have a profound effect on the performance and durability of PEMFCs.

Acknowledgments
The French Région Franche-Comté and IFSTTAR are gratefully acknowledged for their supports through the funding of the Nicolas Noguer PhD thesis.

7. References

[1] Alaswad A, Baroutaji A, Achour H, Carton J, Al Makky A, Olabi AG. Developments in fuel cell technologies in the transport sector. International Journal of Hydrogen Energy 2016; 41(37): 16499-16508.

[2] Tabbi Wilberforce, Alaswad A, Palumbo A, Dassisti M, Olabi AG. Advances in stationary and portable fuel cell applications. International Journal of Hydrogen Energy 2016; 41(37): 16509-16522.

[3] Yousfi-Steiner N, Moçotéguy P, Candusso D, Hissel D. A review on polymer electrolyte membrane fuel cell catalyst degradation and starvation issues: causes, consequences and diagnostic for mitigation. Journal of Power Sources 2009; 194(1): 130-145.

[4] Guoliang Ding, Santare MH, Karlsson AM, Kusoglu A. Numerical evaluation of crack growth in polymer electrolyte fuel cell membranes based on plastically dissipated energy. Journal of Power Sources 2016; 316: 114-123.

[5] Mohsen Mousavi Ehteshami S, Amirhooshang Taheri, Chan SH. A review on ions induced contamination of polymer electrolyte membrane fuel cells, poisoning mechanisms and mitigation approaches. Journal of Industrial and Engineering Chemistry 2016; 34: 1-8.

[6] Junye Wang. Barriers of scaling-up fuel cells: Cost, durability and reliability. Energy, Volume 80, 1 February 2015, Pages 509-521.

[7] Mawardi A, Pitchumani R. Effects of parameter uncertainty on the performance variability of proton exchange membrane (PEM) fuel cells. Journal of Power Sources 2006; 160(1):232-245.

[8] Naga Srinivasulu G, Subrahmanyam T, Dharma Rao V. Parametric sensitivity analysis of PEM fuel cell electrochemical Model. International Journal of Hydrogen Energy 2011; 36(22):14838-14844.

[9] Placca L, Kouta R, Blachot J-F, Charon W. Effects of temperature uncertainty on the performance of a degrading PEM fuel cell model. Journal of Power Sources 2009; 194(1):313-327.

[10] Placca L. Impact des incertitudes sur le fonctionnement des piles à combustible par approche fiabiliste. UTBM - CEA PhD Thesis, Defended on December 17, 2010. 224 pages.

[11] Yuan W, Tang Y, Pan M, Li Z, Tang B. Model prediction of effects of operating parameters on proton exchange membrane fuel cell performance. Renewable Energy 2010; 35(1):656-66.

[12] Noorkami M, Robinson JB, Meyer Q, Obeisun OA, Fraga ES, Reisch T, Shearing PR, Brett DJL. Effect of temperature uncertainty on polymer electrolyte fuel cell performance. International Journal of Hydrogen Energy 2014; 39(3):1439-1448.

[13] Kerdy M, Eid M, Kouta R, Châtelet E. Probabilistic analysis of behaviour and ageing of PEM fuel cell with integration of degradation models and random temperature. Proceeding of the 31st ESReDA Seminar, Smolenice Castle, Slovakia, November 7-8th, 2006. 14 pages.

[14] Fowler M W, Mann R F, Amphlet J C, Peppley B A, Roberge P R (2002) Incorporation of voltage degradation into a generalised steady state electrochemical model for a PEM fuel cell, Journal of power sources 2002; 106:274-283.

[15] Michael Whiteley, Ashley Fly, Johanna Leigh, Sarah Dunnett, Lisa Jackson. Advanced reliability analysis of Polymer Electrolyte Membrane Fuel Cells using Petri-Net analysis and fuel cell modelling techniques. International Journal of Hydrogen Energy, In Press, Corrected Proof, Available online 25 February 2015

[16] Weber AZ, Borup RL, Darling RM, Das PK, Dursch TJ, Gu W, Harvey D, Kusoglu A, Litster S, Mench M, Mukundan R, Owejan JP, Pharoah J, Secanell M, Zenyuk IV. A Critical Review of Modeling Transport Phenomena in Polymer-Electrolyte Fuel Cells. Journal of the Electrochemical Society 2014; 161(12), F1254-F1299.

[17] Noguer N, Candusso D, Kouta R, Harel F, Charon W, Coquery G. A PEMFC multi-physical model to evaluate-the consequences of parameter uncertainty on the fuel cell performance. International Journal of Hydrogen Energy 2015; 40(10):3968-3980.

[18] Noguer N. Aide à l'analyse fiabiliste d'une pile à combustible par la simulation. UTBM - IFSTTAR PhD Thesis, Defended on July 7, 2015. https://www.dropbox.com/l/s/KV7t3Rc1yxwLCokxcr0MJs.

[19] Charon W, Ilchev MC, Blachot JF. Mechanical simulation of a Proton Exchange Membrane Fuel Cell stack using representative elementary volumes of stamped metallic bipolar plates. International Journal of Hydrogen Energy 2014; 39(25): 13195-13205.

[20] Akiki T. Modélisation de la dégradation de la production de puissance d'une PAC suite aux sollicitations mécaniques. UTBM PhD Thesis, Defended on March 3, 2011. 192 pages.

[21] Zhang Z. Modélisation mécanique des interfaces multi-contacts dans une pile à combustible. University of Every-Val d'Essonne, PhD Thesis, Defended on November 30, 2010.

[22] DYMOLA software. http://www.3ds.com/products/catia/portfolio/dymola/overview/

[23] MODELICA language. https://www.modelica.org/

[24] Poirot-Crouvezier JP. Modélisation dynamique des phénomènes hydrauliques, thermiques et électriques dans un groupe électrogène à pile à combustible. Institut National Polytechnique de Grenoble, PhD Thesis, 2000.

[25] Schott P, Baurens P. Fuel cell operation characterization using simulation. FDFC'04 France Deutschland Fuel Cell Conference 2004, Belfort (France), pp. 383-388.

[26] Noiying P, Hinaje M, Thounthong P, Raël S, Davat B. Using electrical analogy to describe mass and charge transport in PEM fuel cell. Renewable Energy 2012; 44:128-140.

[27] Faydi Y, Lachat R., Meyer Y. Thermomechanical characterisation of commercial Gas Diffusion Layers of a Proton Exchange Membrane Fuel Cell for high compressive pre-loads under dynamic excitation. Fuel 2016: 182: 124 - 130.

[28] El Oualid S, Lachat R, Candusso D, Meyer Y. Experimental process to measure the electrical contact resistance of Gas Diffusion Layers under mechanical static compressive loads. AEM2016 Conference. 12-14 September 2016. University of Surrey, England.

[29] Xunliang Liu, Fangyuan Peng, Guofeng Lou, Zhi Wen. Liquid water transport characteristics of porous diffusion media in polymer electrolyte membrane fuel cells: A review. Journal of Power Sources 2015; 299: 85-96.

[30] N. Zamel, X. Li. Effective transport properties for polymer electrolyte membrane fuel cells-with a focus on the gas diffusion layer. Progress in Energy and Combustion Science 2013; 39(1): 111-146.

[31] Jaeman Park, Hwanyeong Oh, Taehun Ha, Yoo Il Lee, Kyoungdoug Min. A review of the gas diffusion layer in proton exchange membrane fuel cells: Durability and degradation. Applied Energy 2015; 155: 866-880.

[32] Rupak Banerjee, Satish G. Kandlikar. Two-phase flow and thermal transients in proton exchange membrane fuel cells - A critical review. International Journal of Hydrogen Energy 2015; 40(10): 3990-4010.

[33] Pauchet J, Prat M, Schott P, Pulloor Kuttanikkad S. Performance loss of proton exchange membrane fuel cell due to hydrophobicity loss in gas diffusion layer: Analysis by multiscale approach combining pore network and performance modelling. International Journal of Hydrogen Energy 2012; 37(2): 1628-1641.

[34] M. Bosomoiu, G. Tsotridis, T. Bednarek. Study of effective transportation properties of fresh and aged gas diffusion layers. Journal of Power Sources 2015; 285:568-579.

[35] Norman JL, Kotz S, Balakrishnan N. Continuous Univariate Distributions. A Wiley-Interscience Publication, 1994. 791 pages. ISBN: 978-0-471-58495-7.

[36] Pillet M. Les plans d'expériences par la method Taguchi. Paris: Organisation of Ed 1999, c1997, ISBN: 2-7081-2031-X.

[37] Goupy J. La methode des plans d'expériences : optimisation du choix des essais et de l'interprétation des résultats. Paris: Dunod, c1988, ISBN: 2-04-018732- 4.

[38] Wahdame B, Candusso D, François X, Harel F, Kauffmann JM, Coquery G. Design of experiment techniques for fuel cell characterisation and development. International Journal of Hydrogen Energy 2009; 34(2):967-980.

[39] Goulet M-A, Khorasany RMH, De Torres C, Lauritzen M, Kjeang E, Wang GG, Rajapakse N. Mechanical properties of catalyst coated membranes for fuel cells. Journal of Power Sources 2013; 234:38-47.

[40] Khorasany RMH, Sadeghi Alavijeh A, Kjeang E, Wang GG, Rajapakse RKND. Mechanical degradation of fuel cell membranes under fatigue fracture tests. Journal of Power Sources 2015; 274:1208-1216.

Figure Captions

Fig. 1. First model layer of the PEMFC simulated in the DYMOLA environment. Examples of key physical phenomena considered in different model sub-layers.

Fig. 2. Schematic representation of the integration process and analysis of the uncertainties in the knowledge model developed under DYMOLA [17].

Fig. 3. Stochastic convergence analysis to determine the minimum number of samples / drawings required to obtain a stable cell voltage.

Fig. 4. Distributions obtained after 2000 drawings (cell simulations in nominal operating conditions).
- On the left side: for the input parameter, i.e. the porosity of the GDL (mean value = 0.6; *CoV*=10%).
- On the right side: for the response, i.e. the cell voltage.

Fig. 5. Example of distributions on the semi-empirical $\beta 5$ input parameter (left) and the response (right) obtained when using the "simple" model only.

Fig. 6. Distribution of the cell voltage in the nominal conditions, for three input distributions:
- Coefficient of variation of 1% (top),
- Coefficient of variation of 5% (middle),
- Coefficient of variation of 10% (bottom).

Fig. 7. Pressure dispersions in the electrode at the cathode side.
- Partial pressure of oxygen (top, left).
- Nitrogen partial pressure (top, right).
- Partial pressure of water vapor (bottom, left).
- Total pressure (bottom, right).

Fig. 8. Dispersion of the pressures in the gas diffusion layer at the cathode side.
- Partial pressure of oxygen (top, left).
- Nitrogen partial pressure (top, right).
- Partial pressure of water vapor (bottom, left).
- Total pressure (bottom, right).

Fig. 9. Evolution of the coefficient of variation for the output (Output *CoV*) versus the FC current, and as a function of the dispersion on the porosity (Input *CoV*).

Fig. 10. Distributions obtained after 2000 drawings (cell simulations in nominal operating conditions).
- On the left side: on the input parameter, the porosity of the GDL at cathode (mean value = 0.6; *CoV*=10%).
- On the right side: on the response, here the membrane resistance.

Table Captions

Table 1. Cell characteristics.

Table 2. Cell nominal operating conditions.

Table 3. Characteristics of the input distribution (GDL porosity).

Table 4. Levels of the factors considered in the design of experiment.

Table 5. Design of Experiments for a load current of 110 A.

Table 6. The effects and interactions of the parameters *T*, *P*, and *CoV* on the voltage at 110 A.

Table 7. ANOVA table computed at 110 A, with *T*, *P*, *CoV* as input factors and with the mean voltage value of the distribution (*M*) as the response.

Table 8. ANOVA table computed at 110 A, with *T*, *P*, *CoV* as input factors and with the standard deviation of the voltage distribution (*E*) as the response.

Table 9. Coefficient of variation for the output (voltage) versus the coefficient of variation for the input (GDL porosity). For different levels of operating parameters (*T*, *P*, and *I*).

Table 10. Table of the effects and interactions of the parameters on the resistance at 110 A.